Biogeosciences Discuss., 5, 2541–2581, 2008
www.biogeosciences-discuss.net/5/2541/2008/

Biogeosciences Discussions

Biogeosciences Discussions is the access reviewed discussion forum of *Biogeosciences*

Sinking rates of particles in biogenic silica- and carbonate-dominated production systems of the Atlantic Ocean: implications for the organic carbon fluxes to the deep ocean

G. Fischer[1] **and G. Karakas**[2]

[1]Faculty of Geosciences and MARUM, University of Bremen, Klagenfurter and Leobener Strasse, 28359 Bremen, Germany
[2]Alfred-Wegener-Institute for Polar and Marine Research, Columbusstrasse, 27568 Bremerhaven, Germany

Received: 29 February 2008 – Accepted: 29 February 2008 – Published: 16 June 2008

Correspondence to: G. Fischer (gerhard.fischer@uni-bremen.de)

Published by Copernicus Publications on behalf of the European Geosciences Union.

Abstract

The flux of materials to the deep sea is dominated by larger, organic-rich particles with sinking rates varying between a few meters and several hundred meters per day. Mineral ballast may regulate the transfer of organic matter and other components by determining the sinking rates, e.g. via particle density. We calculated particle sinking rates from flux patterns and alkenone measurements applying sediment trap experiments from the Atlantic Ocean. We obtained higher particle sinking rates in carbonate-dominated production systems, both regionally and seasonally. During a summer coccolithophorid bloom in the Cape Blanc coastal upwelling off Mauritania, sinking rates reached almost 570 m per day, most probably due the fast sedimentation via zooplankton fecal pellets. During the recurring winter-spring blooms off NW Africa and in opal-rich production systems of the Southern Ocean, sinking rates of larger particles, most probably diatom aggregates, appeared to be lower. Although a tight and overall coupling between dust supply and particle sinking rates was not observed, it remains noticeable that the highest sinking rates occurred mostly in the dust-rich ocean regions off NW Africa. We obtained increasing sinking rates with depth. By using a seven-compartment biogeochemical model, it was shown that deep ocean organic carbon fluxes at a mesotrophic sediment trap site off Cape Blanc can be captured fairly well using seasonal variable particle sinking rates. Our model provides a total organic carbon flux of 0.29 Tg per year down to 3000 m off the NW African upwelling region between 5 and 35° N.

1 Introduction

The functioning of the biological pump plays a critical role in the discussion about glacial-interglacial pCO_2 variations measured in ice cores as well as in the evaluation of future climate scenarios. At highest efficiency, it may draw down atmospheric pCO_2 to about 150 μatm, at lowest efficiency, in a biologically dead ocean, the value may be as

high as 415 μatm (Broecker, 1982). The transfer of particulate organic carbon to depth in the modern ocean shows considerable regional and temporal variability in the fraction of primary production (5 to 25%) that is exported to depth. Despite considerable progress in recent years, this variability is far from being completely understood, mainly due to a lack of knowledge of relevant meso- and bathypelagic processes (e.g. Boyd and Trull, 2007).

The efficiency of carbon transfer to depth is influenced by three major processes (de la Rocha and Passow, 2007): a) the amount of primary production in the photic layer, b) the velocity of which organic carbon sinks down, and c) the rate of POC decomposition. All these processes impact on ocean biogeochemistry. Small zoo- and phytoplankton sinks predominantly as larger composite particles, mainly fecal pellets or marine snow aggregates (Alldredge and Silver, 1988), owing typical sinking velocities between 50 and 250 m d^{-1}. These particles are widely considered as major transport vehicles of materials to the deep sea (e.g. Smetacek, 1985; Pilskaln and Honjo, 1987). However, sinking rates of both particle types display a large variation which cannot be explained yet. Direct field measurements are still rare and many values originated from laboratory experiments (e.g. Ploug et al., 2008), coastal-near regions or from surface waters only (Alldredge and Silver, 1988; Angel, 1984). Increasing sinking rates with depth provide indirect evidence of changes in particle characteristics (e.g. porosity and/or density) in the water column and particle composition (Berelson, 2002). They may be responsible for the variable organic carbon flux attenuation curves in the water column (e.g. Francois et al., 2000; Boyd and Trull, 2007).

Mineral ballast is an important issue in the discussion about particle formation, sinking rates and carbon transfer to the deep ocean (Ittekkot, 1993; Armstrong et al., 2002; Francois et al., 2002; Klaas and Archer, 2002; Passow, 2004). However, little is known about the mechanisms behind the ballast theory and empirical findings do not show cause and effect as pointed out by Passow (2004). She suggested that POC fluxes determine fluxes of ballast minerals and that marine snow aggregates scavenge mineral particles both of biogenic and lithogenic origin until their carrying capacity is reached.

BGD
5, 2541–2581, 2008

Armstrong et al. (2002) argued that the fraction of POC reaching the deep ocean is chemically protected from degradation by mineral particles. On the other hand, differential sinking speeds of larger particles could also explain field observations and the ballast theory (Klaas and Archer, 2002; Francois et al., 2002). The latter authors speculated that remineralisation in the twilight zone of the low-latitude oceans is relatively low due to high carbonate mineral availability which may constitute dense and fast sinking fecal pellets. Fecal pellets may be the main vector for sedimentation of coccolithophorids in the ocean (de La Rocha and Passow, 2007). In contrast, high-latitude oceans with high export of marine snow aggregates which are formed preferentially by diatoms and have a labile nature may be characterized by reduced particle sinking rates and low organic carbon transfer rates. Such scenarios would correspond to the overall picture that fecal pellets have generally higher sinking rates (~10–2700 m d^{-1}, Angel, 1984, 1989; Turner, 2002) than the less denser and TEP-rich marine snow aggregates (1–368 m d^{-1}; Alldredge and Silver, 1988) which may be even retained in the surface layer for several days (Riebesell, 1992).

The role of lithogenic material, i.e. dust as a major carrier for organic carbon is discussed controversially (e.g. Boyd and Trull, 2007). Globally, the role may be irrelevant as pointed out by Francois et al. (2002). Culture studies have shown that lithogenic material could even decrease the downward flux of phytoplankton biomass (Hamm, 2002). According to Berelson (2002), particle sinking rates estimated from sediment trap studies appear to be not impacted by the lithogenic contents of particles. He concluded that sinking velocities of particles increase with depth, however, the database applied in this study was not from the same locations.

The variation in particle characteristics across different production systems is an issue that biogeochemical models have to confront. A bigger challenge for modellers nevertheless is the representation of particle transformations in the water column as they sink. Biogeochemical models (e.g. Gruber et al., 2006) have traditionally used prescribed particle sinking velocities that are at least several orders of magnitude smaller than the velocities estimated from deep water sediment trap recordings. This incon-

sistency must be taken care of by appropriate algorithms, which ensure reconciliation of surface ocean productivity with deep water fluxes. Coagulation theory attempted to formulate particle aggregation and disaggregation and achieved significant progress to explain these transformations in the water column (see Jackson, 2005, for a review). In a rare application, Gehlen et al. (2006) implemented an aggregation kernel into a 3-D biogeochemical ocean model to study the biological soft tissue pump. She showed that an aggregation model did not improve subsurface POC fluxes relative to the simple, 2-particle-size-classes model with prescribed sinking rates, despite Jackson's (2001) scepticism about simple parameterisations to represent the effect of coagulation in biogeochemical models.

Here we investigate if different production systems show differences in particle sinking rates as hypothesized by Francois et al. (2002). We also examine the role of coccolithophorid carbonate as major ballast mineral, not total carbonate (mainly coccolithophorids and planktonic foraminifera) as done by Francois et al. (2002) and Klaas and Archer (2002). We use alkenone-derived sea surface temperatures (SSTs, Müller and Fischer, 2001) to assess coccolithophorid-associated sinking rates of particles in the meso- and bathypelagic. We will use particle fluxes from different sediment trap levels to approximate average particle sinking rates in the deeper water column and to test the hypothesis of increasing sinking rates with depths (Berelson, 2002). Multi-year collections of particles also allow an assessment of the seasonal and interannual variability of particle sinking rates.

We then extend our investigation to explore the possibility of representing particle fluxes in the deep water by using a simple regional biogeochemical model with prescribed, averaged sinking velocities. We subsequently show how seasonal variation of particle sinking rates control deep water carbon fluxes. The model was setup for the Cape Blanc filament region in the NW African upwelling system, which hosts significant export production with some biogenic opal and high carbonate production. Because size spectrum and sinking speeds of particles can be simulated fairly well with two size classes (Gehlen et al., 2006), a biogeochemical model with two detritus compartments

was used for modeling particle fluxes. The biogeochemical model was coupled to an ocean circulation model and was run with real-time forcing data for the measurement period. The results are compared to the satellite-derived imagery and deep sediment trap recordings.

2 Material and methods

2.1 Sediment trap collections and analysis

Large-aperture time-series sediment traps of the Kiel-type were used for particle collection at our study sites (Fig. 1). They were equipped with 20 cups and had openings of 0.5 m^2 (Kremling et al., 1996). Swimmers were removed by hand using forceps and the material was wet-sieved through a 1 mm nylon mesh. Particle flux data from all sites refer to the size fraction of smaller than 1 mm. The homogenized samples were split into sub-samples on which further analysis was performed. Mass flux was determined by weighing the sub-samples. Total carbon, organic carbon and nitrogen were obtained by combustion with a HEREAUS-CHN-analyzer. Organic carbon was measured after removal of carbonate with 2N HCl. Carbonate was determined by subtracting organic carbon from total carbon, the latter being measured by combustion without a pre-treatment with 2N HCl. Biogenic opal was measured according to Müller and Schneider (1993) using a sequential leaching technique with 1M NaOH as dissolving agent. The lithogenic fraction was calculated as follows: Lithogenic = Total flux – opal – carbonate – 2*C_{org}. Alkenone concentrations and calculated SST were done according to Müller and Fischer (2001).

To avoid problems with the trapping efficiency, which appears to be lower in the surface and subsurface waters (Yu et al., 2001; Scholten et al., 2001), we used flux data from deeper traps (mostly 700 m to about 1000 m) to circumvent strong undersampling. On the other hand, we intended to avoid depths where lateral input of material enhanced particle flux as had previously been observed in the Canary Island region

BGD
5, 2541–2581, 2008

(e.g. Neuer et al., 1997, 2002). For a detailed description of currents velocities and directions and the discussion of trapping efficiencies see Fischer et al. (1996a, site CB, 2000, 2002, Atlantic and Southern Ocean).

2.2 Estimation of particle sinking rates

To calculate sinking rates we used sediment traps from two different water depths (about 1000 m water depths and 500 m above the seafloor, Table 1). Two approaches were applied, both using seasonal flux data to capture potential seasonal changes in particle sinking rates. The first one compared the time shift of major flux peaks of total mass, divided by the distance between both traps by half the sampling interval (at a one-cup shift). The second approach followed the method of Berelson (2002) who attempted to find the best fit between total fluxes at two water depths by shifting the complete time series by one or two sampling intervals. A comparison of both methods showed a close relationship with a correlation coefficient of R^2=0.66 (N=35) and correlation method provides slightly higher sinking rates. We further calculated sinking rates of alkenone-associated particles, mainly coccolithophorids, by determining the time shift between maxima/minima of measured SSTs (weekly, IGOSS; Reynolds and Smith, 1994; http://ingrid.ldgo.columbia.edu/SOURCES/.IGOSS/data_products.html) and alkenone-derived temperatures obtained from trap samples (see Müller and Fischer, 2001, 2003) or by a comparison between alkenone-based temperatures from two different trap levels.

The estimated sinking rates calculated for various seasons must be regarded as the lowest estimates due to the relatively high time resolution for collection (Table 1). The estimated sinking rates are dependent on the sampling intervals which range from 9.5 to 30 days (average 19.6 days, Table 1). To account for extreme differences in sampling intervals between the study sites, we normalized our sinking rates to a mean value of 19.6 days. The results are shown in Fig. 2 for both methods, whereby the major peak method provided a larger data scatter (r^2=0.54, N=38) and a regression line quite far from the 1:1 line compared to the correlation method (r^2=0.69, N=36). For plot-

ting sinking rates in relationship to other parameters we therefore applied normalized sinking rates derived from the correlation method.

2.3 Modeling particle fluxes

Regional Ocean Modelling System (ROMS) coupled to a seven-compartment biogeochemical model was applied to study deep water fluxes and their seasonal variation in the Cape Blanc region. ROMS is a well established terrain-following, hydrostatic, primitive equation ocean circulation model with orthogonal curvilinear horizontal coordinates. The numerical algorithms of the code are described in a series of papers by Shchepetkin and McWilliams (1998, 2003, 2005). The novelty in these algorithms is a split-explicit hydrodynamic kernel that treats baroclinic and barotrophic modes in such a way that ensures tracer conservation and prevents errors associated with unresolved barotrophic processes. Barotrophic fields are temporally averaged with a cosine-shape filter before replacing the values calculated with a longer baroclinic time step. By redefining barotrophic pressure-gradient terms according to the changes in local density fields, accuracy of the scheme is improved without compromising from computational efficiency.

The biogeochemical model was a classical, nitrogen based, NPZD type, which was developed and defined in detail by Gruber et al. (2006). The model comprises seven compartments; nitrate, ammonium, phytoplankton, zooplankton, small and large detritus, and a dynamic phytoplankton chlorophyll to carbon ratio. Apart from zooplankton, all particulate compartments sink, which is modelled explicitly. Small particles are represented by a slow settling small detritus pool. Small detritus and phytoplankton coagulate to form large detritus, which sink faster. Coagulation is parameterised according to a particle density function based on the assumption that coagulation is proportional to particle concentration. Parameter values of the biogeochemical model are given in Gruber et al. (2006). These values remained unchanged in our configuration apart from the remineralisation rates of small and large detritus, specific coagulation rate between small detritus and phytoplankton, and large detritus sinking velocity. While

remineralisation rates for small and large particles were set to $0.18\,d^{-1}$ and $0.06\,d^{-1}$, respectively, particle coagulation rate was specified as $0.07\,d^{-1}\,(mmol\,m^{-3})^{-1}$.

Our model domain covers the region between 5° to 41° N and 30° to 5.5° W, and has a resolution of 12 km. GEBCO data (IOC, IHO and BODC, 2003) was used to produce model bathymetry. In the vertical 32 s-coordinate levels are set with increasing resolution towards the surface. World Ocean Atlas 2001 (WOA2001) (Stephens et al., 2002; Boyer et al., 2002) climatology is used for the initialisation of the model from rest in January. Monthly means of this climatology is employed along the lateral boundaries to prescribe temperature, salinity, nutrient and momentum fluxes. The model is forced with monthly averaged COADS (Comprehensive Ocean-Atmosphere Data Set) for the heat, fresh water and momentum fluxes (da Silva et al., 1994) during spin-up. After 3 years of spin-up the model was forced by 6-hourly NCEP reanalysis-2 data (Kanamitsu et al., 2002) for the years 2002 and 2003, i.e. during the time sediment trap data were collected at the mesotrophic CB13 deployment site off Cape Blanc.

Particles sink into the ocean's floor in a complex process with varying sinking velocities depending on their constituents, size, shape, porosity and way of formation (Kriest, 2002). A variety of sinking velocities have been observed at Cape Blanc site (see Table 3). By looking into the delay between chlorophyll maxima at the surface and the corresponding sedimentation peaks in the trap, Helmke et al. (2005) calculated a mean downward particle flux velocity of $75\,m\,d^{-1}$ at this site. We therefore set the sinking velocity of large particles to $75\,m\,d^{-1}$ in the model setup. Due to the seasonal variation (see Sect. 3.4) we increased sinking velocity by a factor of 2 below the euphotic layer in summer, which corresponds to trap samples #3 through #5.

3 Results and discussion

3.1 Sinking rates determined from total flux patterns

Sinking rates of particles determined from sediment trap samples ranged from 73 to 741 m d^{-1} applying the correlation method, with a mean value of around 210 m d^{-1} (Table 1). At site CV (Cape Verde Islands, Fig. 1), we obtained a large interannual variation in sinking rates obviously due to exceptionally different sampling intervals of 9.5 and 25 days. Therefore, this range must be regarded with caution. Normalized sinking rates provided a range of 107 to 395 m d^{-1} in which values from site CV match well. These normalized values are within the range for larger particles given by Alldredge and Silver (1988) and Angel (1984, 1989), which were derived to a large part from laboratory experiments. In Fig. 3, the latitudinal distribution of normalized sinking rates is plotted showing also the means derived from the correlation method. Lowest sinking rates were obtained in the Southern Ocean, at the Walvis Ridge and in the western Equatorial Atlantic, highest values were found in the eastern Equatorial Atlantic and off NW Africa.

Mean normalized sinking rates are given in Fig. 4d together with the composition of particles (% of total annual mass) from the upper trap levels (Table 1) and the mean sinking rates from Berelson (2002) for the Pacific Ocean (158 m d^{-1}) and the Arabian Sea (230 m d^{-1}) which fit into our distribution pattern. We observe highest rates at and south of the equator, in particular in the eastern Atlantic which correspond to highest organic carbon and carbonate contents. Consequently, biogenic opal contents remain low there. This finding corresponds at first sight to the global distribution of organic carbon transfer efficiency which is higher in carbonate (equatorial regions) compared to biogenic opal production systems (polar or subpolar regions). Francois et al. (2002) speculated that this might reflect a fundamental difference in the particle transport mode, i.e. fast sinking fecal pellets in carbonate vs. slowly sinking diatom aggregates in opal production systems. Diatoms are the predominant producers of phytoplankton marine snow aggregates (Alldredge and Gotschalk, 1989) and are ca-

BGD
5, 2541–2581, 2008

pable to produce large amounts of relatively light TEP (Alldredge et al., 1993). Marine snow aggregates or flocs produced by diatoms have sinking rates in the order of 100 to 150 m d^{-1} (Smetacek, 1985; Billet et al., 1983; Alldredge and Gotschalk, 1989), thus corresponding to our mean value for the Southern Ocean (157 m d^{-1}, Table 1). However, in coastal setting of the Ross Sea, diatom aggregates may have sinking rates higher than 288 m d^{-1} as measured by Asper and Smith (2003). Diatoms in the Southern Ocean may be also transported via euphausiid fecal pellets (Wefer et al., 1988) which have sinking rates of several hundreds of meters per day (Fowler and Small, 1972; Cherry et al., 1978).

Marine snow aggregates formed by coccolithophorids, the major primary producers of carbonate in the ocean (Berner and Honjo, 1981; Schiebel, 2002) have not yet been observed (de la Rocha and Passow, 2007). At a site in the Panama Basin, mass sedimentation of a single coccolithophorid species to the deep sea has been observed by Honjo (1982), whereby the individual cells appeared to be embedded in mucus and the material descended with a mean rate of about 65 m d^{-1} only. In most cases, however, these organisms appear to sink within rather densely packed fecal pellets (Honjo, 1976; Knappertsbusch and Brummer, 1995; Fischer et al., 1996b). Fecal pellets have generally higher sinking rates (10–2700 m d^{-1}, mean around 500 m d^{-1}; Angel, 1984, 1989; Fowler and Knauer, 1986; Cadée et al., 1992; Turner, 2002) than the less denser marine snow aggregates (16–26 m d^{-1} from Pilskaln et al., 1998; 10 m d^{-1} (mean); from Dierks and Asper, 1997; 1–36 m d^{-1} from Asper, 1987; 100–150 m d^{-1} from Smetacek, 1985; Billet et al., 1983; Alldredge and Gotschalk, 1989). However, a close relationship between particle sinking rates and carbonate content was not found in our study. This may be explained by a variable and largely unknown composition of total carbonate in the modern ocean, i.e. mainly coccolithophorids vs. planktic foraminifera (see below). Total carbonate appears to be mostly composed of coccolithophorids in the modern ocean, but foraminifera may contribute up to 50–70% of the total carbonate flux (Berner and Honjo, 1981; Schiebel, 2002). In contrast to small coccolithophorids, foraminifera appear to sink mainly individually, not within larger particles and should

not be included into the carbonate fluxes when discussing carbonate ballasting effects on organic carbon.

Lithogenic contents of particle fluxes from the entire Atlantic do not show an overall and clear corresponding distribution to particle sinking rates. However, particle sinking rates decrease from about 315 to 183 m d^{-1} in the eastern Atlantic in a southward direction (Table 1), concomitant with a decrease in the flux of lithogenic materials (Fischer and Wefer, 1996). The northern sites (EEA 2° N, EEA 0°) having relatively high sinking rates (315–400 m d^{-1}) are strongly influenced by the migration of the ITCZ bringing fine-grained lithogenic components (dust) into the oceanic environment. As the sinking rates are mostly derived from winter and spring sedimentation, the time of the southernmost extension of the ITCZ, an impact on particle composition may be plausible. Consequently, at the two northernmost sites, particle loading via lithogenic components (Ittekkot, 1993) may have occurred, thus increasing particle sinking rates.

Surprisingly, particle sinking rates are relatively high in the western Equatorial Atlantic, in particular at the oligotrophic site WEA 7° S with a mean of 302 m d^{-1} (Table 1, Fig. 3). This area is remote from the influence of dust supplied by the ITCZ and the sinking rates were calculated mostly from summer data when the ITZC is far north between 10 and 15° N. Instead, this site with the highest sinking rates (454 or, normalized, 394 m d^{-1}) is characterized by the highest total carbonate content (70%) combined with very low lithogenic components (around 7%). One problem with the ballast hypothesis (e.g. Francois et al., 2002) is that the global relationship between organic carbon and carbonate is based on total carbonate rather than, as it should be, on coccolithophorid carbonate. These organisms are thought to be transported mainly within fast sinking pellets, thus transporting organic carbon and other organic components (e.g. chlorophyll derivates) very efficiently to greater depth (Fischer et al., 1996b). In studies using alkenones which are thought to be produced mainly by coccolithophorids, we calculated sinking rates associated primarily with these organisms (Müller and Fischer, 2001, 2003).

3.2 Coccolithophorid-associated particle sinking rates

This approach allows the estimation of particle sinking rates in the bathypelagic by comparing trap results from two different levels but also the assessment of average sinking rates in the mesopelagic zone by comparing measured SST (IGOSS data set) with the reconstructed temperatures of the upper traps derived from alkenone measurements (Müller and Fischer, 2001, 2003) (Fig. 5). Sinking rates from the mesopelagic zone are valuable as they document the sum of aggregation-disaggregation processes and the complexity of food web structure occurring in this zone. We obtained unusually low sinking rates of $9\,m\,d^{-1}$ in the Southern Ocean (site PF3, 0–613 m water depth), probably due to a long range lateral displacement of particles within the deep-reaching, constantly eastward flowing Antarctic Circumpolar Current (ACC) which has relatively high current velocities (Müller and Fischer, 2003). Advection of water masses and transport of larger particles over laterally significant distances from their point of origin is also described by Gorsky et al. (2003).

Not only the sinking rates estimated from total particle fluxes for the bathypelagic are lower in the Southern Ocean (mean: $157\,m\,d^{-1}$, Table 1) compared to the tropical and subtropical environments but also coccolithophorid-associated carbon appears to sink rather slow through the mesopelagic. This suggests that coccolithophorids are not everywhere transported rapidly downwards via fast sinking fecal pellets. A long-range transport is also proposed from the sinking rates of coccolithophorid-associated particles in the eastern equatorial Atlantic (site EA8, Table 1; Müller and Fischer, 2003), with mean sinking rates in the order of $13\,m\,d^{-1}$ for the water column between the surface and 598 m. Higher values of $48\,m\,d^{-1}$ were recorded for the Benguela System (trap WR-2-4), however, between the surface and 1648/1717 m. At site NU2 off Namibia, $45\,m\,d^{-1}$ were estimated between the surface and 2516 m. These observations indicate increasing sinking rates with depth for alkenone-containing particles. Sinking of coccolithophorid mats containing mucus in the Panama Basis was in the order of $65\,m\,d^{-1}$ (Honjo, 1982), thus being well within our range of values discussed above

BGD
5, 2541–2581, 2008

and below. Sawada et al. (1998) found sinking rates of alkenone-associated particles in the western Pacific off Japan of 145–290 m d^{-1}, but for a water column of 8000 m.

A detailed study was performed in the upwelling filament off Cape Blanc (Müller and Fischer, 2001, and unpublished data), indicating the high interannual variability of sinking rates and associated transport processes. We obtained sinking rates for the mesopelagic between 15 and 73 m d^{-1} (Table 2), being within the range of values from the Atlantic Ocean described above. These relatively low rates might indicate a significant lateral displacement of larger particles from their point of origin, most probably from the coast (e.g. Karakas et al., 2006). Values between the surface and the deep traps were between 73 and 100 m d^{-1} for the deployments CB-1-3 and CB-13, suggesting increasing sinking rates with depth (see also below). During deployment CB-4 in summer 1991, however, sinking rates were 356 m d^{-1} (Table 3). Between the upper trap and the deeper trap level, sinking rates were even as high as 566 m d^{-1}. During this year, organic carbon transfer and the alkenone fluxes to depth were extraordinary high (Müller and Fischer, 2001; Fischer et al., 2008), although production at the surface was assumed to be even decreasing. When calculating the coccolithophorid flux from total carbonate flux (by counting and weighing planktic foraminifera and pteropods), we found that almost all carbonate (95%) was supplied by coccolithophorids in 1991. In contrast, during deployment CB-3 (1989), we obtained a contribution of coccolithophorid-carbonate in the order of only 65%. We assume that an episodic pulse of a coccolithophorid bloom in 1991 (CB-4) was exported rapidly in a vertical direction leading to an effective transfer of carbon via fast sinking fecal pellets.

We collected mesozooplankton fecal pellets densely packed with coccolithophorids at the ESTOC site in the Canary Current in 1992. They were able to transport rather fresh organic detritus to greater depth providing a perfect correspondence between seasonal organic carbon and carbonate fluxes (Fischer et al., 1996b). In addition, we found 1000 μm long densely packed macrozooplankton fecal pellets at a more coastal site off Cape Blanc ($CB_{coastal}$-2, unpublished data) which contain large amounts of coccolithophorids and which sink with rates of about 750 m d^{-1} (M. Iversen, unpublished

data). Coccolithophorids being densely packed within quite fast sinking fecal pellets (around 150' m d^{-1}) were described by Knappertsbusch and Brummer (1995) from the North Atlantic near NABE 48° N. Zooplankton fecal pellets with coccolithophorids were also described from the Equatorial Pacific and had sinking rates of 150 m d^{-1} (Honjo, 1976). These values are quite close to our average coccolithophorid-associated sinking rates for the entire water column off Cape Blanc which were around 160 m d^{-1} (Table 3). But our peak value of 566 m d^{-1} appears to be also realistic when considering sinking rates given by Cherry et al. (1978, 50–950 m d^{-1}), Fowler and Small (1972, 126–862 m d^{-1}) or Cadée et al. (1992, 50–800 m d^{-1}). Our studies suggest that the mode of particle transport which determines particle sinking rates may be more important for the amount of carbon reaching the deep sea than primary production in the surface layer (Armstrong et al., 2002). Consequently, organic carbon fluxes or sediment accumulation rates cannot be easily used to estimate modern or past primary production as pointed out by Francois et al. (2002).

3.3 Increasing sinking rates in the water column

Sinking rates derived from alkenone analysis and SST measurements suggest an increase in the water column, e.g. from 15 to 263 m d^{-1} at site CB-3, 73 to 566 m d^{-1} at site CB-4 and 65 to 125 m d^{-1} at site CB-13. All these values from the deeper water column fall within the range of sinking rates derived from the flux patterns, pointing to almost similar values for total material and coccolithophorid-associated carbon and carbonate. In Fig. 5, we plotted the latitudinal distribution of sinking rates from shallower depths (derived from alkenones, Tables 2 and 3) and those from the deeper water column taken from flux comparisons (Table 1). All values from the deeper water column exceed the sinking rates from shallower depths.

Increasing sinking rates of particles have important implications for the degradation of organic carbon and particle remineralisation rates in general. Studies modelling particle transport paths currently operate with fixed sinking rates for the entire water column (e.g. Karakas et al., 2006; Gruber et al., 2006). Lower sinking rates in the

mesopelagic zone (e.g. around 50 m d^{-1} off Cape Blanc, Table 2) may be explained by rather fresh material containing high amounts of organic material combined with relatively low contents of ballast minerals. In the mesopelagic, material may be processed through complex food webs (Legendre and Rivkin, 2002), thus increasing the residence time of materials in this part of the water column. Higher sinking rates in the bathypelagic may be caused by a loss of light organic materials (Berelson, 2002) and a relative increase in ballast minerals. It is known from studies in the deeper water column that the amount of suspended material, e.g. lithogenic components or coccolithophorids (de La Rocha and Passow, 2007) from the sea floor but also from the shelf (e.g. Karakas et al., 2006) may be enhanced and might be incorporated into larger particles (Nowald et al., 2006), thus increasing particle sinking rates.

3.4 Seasonally changing particle sinking rates

In the coastal upwelling setting off Cape Blanc, an E-W transect of surface chlorophyll from SeaWiFs and sediment trap data from deployment CB-9 were used to track the seasonal chlorophyll signals, to determine the source region of particles settling through the water column and to study the relationship between chlorophyll and deep ocean organic carbon fluxes (Helmke et al., 2005). We applied these data to calculate seasonal sinking rates of particles between the surface and 3600 m water depths (CB-9 deployment). We obtained higher sinking rates of about 120 m d^{-1} during the late summer/early fall season when coccolithophorid production was enhanced; during the winter-spring bloom with enhanced biogenic opal sedimentation, sinking rates where only around 90 m d^{-1}. A similar pattern is found for the CB-13 deployment (Fig. 6), applying total flux data from the upper (1228 m) and the lower trap (3606 m). The winter-spring peak measured with the upper trap appeared two cups later in the deep trap where the particle fluxes are almost doubled, pointing to an additional particle source, most probably at the coast (Karakas et al., 2006). This delay translates into a sinking rate of 63 m d^{-1} during the winter-spring bloom. The carbonate-dominated summer

sedimentation in the mesopelagic zone is almost perfectly reflected in the deep trap with some reduction in magnitude, as expected, but without any time shift, suggesting particle sinking rates of 250 m d^{-1}.

3.5 Simulated chlorophyll and deep water fluxes

The model produced physical and biogeochemical characteristics of the upwelling system reasonably well. The simulated hydrodynamic fields are presented by Karakas et al. (2006) and Marchesiello and Estrada (2007). Herein, we explicitly focus on biogeochemical properties. Figure 7 shows annual surface chlorophyll fields for the year 2002 inferred from SeaWiFS and that of our simulation. Despite its relatively coarse resolution, the surface chlorophyll distribution could be reproduced to a great extent. The model shows a slightly exaggerated offshore chlorophyll concentration to the north of Cape Juby, in the north and off Cape Verde in the south. In these locations, the 0.4 mg m^{-3} contour line in the model is around 100–150 km farther offshore than the one in the SeaWiFS data. Off Cape Blanc, on the other hand, which is the region of our interest, the spatial distribution is very similar. The study site CB for instance, where sediment data are recorded, lies under 0.4 mg m^{-3} contour line both in satellite data and modelled fields. Simulated near shore values on the other hand appear to be weaker than remotely recorded data. While relatively coarse grid resolution could be one reason for this anomaly, the quality of remote sensing data in coastal regions could be another, which has been questioned in a number of studies (e.g. Gohin et al., 2002; Lavender et al., 2004; Harding et al., 2005).

In Fig. 8a and b, we compare the seasonal surface chlorophyll from the simulation to that acquired by SeaWiFS. The seasonal variation on the whole is retrieved well by the model solutions. The winter-spring bloom differentiates itself with elevated chlorophyll concentrations in these seasons over large areas of the surface ocean. However, the onshore-offshore chlorophyll gradient in the model does not appear as steep as the observed one. There also exist underestimations (mostly near the coast) and overestimations (to the north of Cape Juby, in spring and winter) of the model. The use

of fine temporal resolution forcing nonetheless is proved to be worthwhile. The model performs remarkably well in winter by reproducing offshore extensions of 0.8 mg m^{-3} contour off Cape Blanc and off Cape Timiris as in the satellite data. Although below the observed concentrations, the summer filament off Cape Blanc is also seen in the model solution. At site CB, very similar chlorophyll concentrations were produced except in autumn. In this season, the model solution (0.11 mg m^{-3}) underestimated the observed value (0.3 mg m^{-3}) at this station by a factor of more than two.

The seasonal variation of surface biomass is successfully mimicked in the deep water organic carbon fluxes. Figure 9 illustrates modelled fluxes against those recorded by the sediment trap at station CB in 3606 m depth. One has to take into consideration that temporal variability and amount of particles sinking into ocean's floor at a particular station can only be reproduced by capturing filaments and patchiness of the flow field in the right time scales, which transport the biogeochemical properties. We believe that although slightly underrated in winter 2003, the general pattern and carbon mass are notably well calculated by the model. It is also worth mentioning that even though particles of different origin sink in different seasons, setting seasonal sinking velocity makes prediction of deep water fluxes possible, despite the fact that the model has one phytoplankton compartment.

We must note that the sinking velocities specified in this study are the mean rates over the entire water column, which give reasonable flux predictions in the deep sediment trap at 3606 m depth. The flux comparison with the upper trap do not show good correlation (data not shown) which may be due to the changing sinking velocities in the water column and /or decreased collection efficiency of shallower sediment traps (Yu et al., 2001; Scholten et al., 2001). It is very unlikely that simple parameterisations can represent the variation in particle characteristics. Biogeochemical models therefore must eventually involve particle aggregation and disaggregation if they are expected to predict flux variations.

Helmke et al. (2005) applied a linear regression model within a box area from 5° N to 35° N and 5° W to 35° W in order to estimate the total flux of organic carbon down to

1000 m depth and came up with values ranging between 1.1 Tg and 2.6 Tg per year. During the period from May 2002 until April 2003, our model calculations give a total organic carbon flux of 292 Gg down to the 3000 m depth contour line off the NW African upwelling region between 5° N and 35° N. Considering the fact that modelled particles, with a remineralisation rate of 0.06 d^{-1} and sinking velocity of 75 m d^{-1}, lose approximately 80% of their mass between 1000 m and 3000 m depth, our value compares well with the estimations given by these authors.

4 Summary and conclusions

We found enhanced particle sinking rates in carbonate-rich production systems which are additionally influenced by dust supply in the equatorial and the eastern North Atlantic. This might reflect a major transport mode for coccolithophorids within densely packed fecal pellets which are frequently found in the material collected by sediment traps. The significance of lithogenic particles for particle sinking rates could not be clearly demonstrated but the high sinking rates off NW Africa remain noticeable. A longer residence time of particles and generally lower sinking rates were obtained in diatom-dominated production systems in the southeast Atlantic and the Southern Ocean as well as during spring blooms in the eastern North Atlantic. We generally obtained lower particle sinking rates in the mesopelagic zone which might reflect the sum of aggregation and disaggregation processes in the twilight zone as well as reduced vertical sinking due to stronger currents in the surface and subsurface layer. Particle sinking rates increase with depth as suggested by Berelson (2002), most probably due to a loss of relatively light organic-rich materials and increased scavenging of suspended mineral particles, both of which would lead to higher particle densities. Our mean sinking rates were highest in the North Atlantic, decreasing slightly southwards (Tables 1 and 3). Average values of alkenone-associated particles were 51 m d^{-1} and 318 m d^{-1} in the upper and lower water column, respectively, thus being well within the range of other studies (e.g. Alldredge and Silver, 1988; Sawada et al., 1988) (Table 3).

BGD
5, 2541–2581, 2008

Many models that try to reproduce particle fluxes and distributions in the water column apply consistent sinking rates in the order of 5–20 m d^{-1}, which are in certain occasions capable to mimic observations in the surface or near-surface layers of the water column, e.g. particle profiles obtained by optical systems (Karakas et al., 2006). However, their capability is limited in the deeper layers due to the small settling velocities. Particle sedimentation has an episodic nature (e.g. Fischer et al., 1996b), which is rarely captured by studies with optical systems because they provide only spot observations over a very short time period of the year. Particle cameras apparently record more the normal distribution of particles in the water column (e.g. mid-water maxima off the shelves, Karakas et al., 2006; Nowald et al., 2006), with larger particle volumes being suspended or sinking slowly. Nevertheless, in one particle profile off NW Africa (Nowald et al., 2006), we were able to capture such an episodic sinking event occurring in spring.

We showed that it was possible to estimate organic carbon fluxes in the deep layers of the ocean to a good degree of accuracy with a simple biogeochemical model once realistic, mean sinking and remineralisation rates are prescribed. This requires a review of parameterisations assigned to biologically produced particles in most biogeochemical models especially when regional studies are involved. A seasonal changing flux velocity between 75 m d^{-1} and 150 m d^{-1} delivered us a satisfactory agreement of simulated values with recorded ones at the Cape Blanc site. However, variation of particle fluxes along the water column can only be represented by elaborate biogeochemical models that incorporate coagulation theory and changing particle characteristics. Processes of disaggregation resulting from shear, zooplankton feeding or fragmentation due to zooplankton must be taken into account. For a better mathematical representation of these processes, further experimental and observational studies are needed.

BGD
5, 2541–2581, 2008

Acknowledgements. We thank the masters and crews of RV METEOR, RV Maria S. MERIAN, RV POLARSTERN and RV POSEIDON for their competent assistance during the deployments and recoveries of the mooring arrays. Thanks are also due to N. Nowald, G. Ruhland, V. Ratmeyer and G. Meinecke (MARUM, Bremen) for their field work and support. For laboratory analysis, we are indebted to M. Klann, R. Kreutz and H. Buschhoff. A large part of the data were collected during the SFB 261 programme (1989–2001, G. Wefer) conducted in the Atlantic Ocean and we would like to thank the Deutsche Forschungsgemeinschaft for funding. This is publication of the Research Center Ocean Margins (RCOM) and the Marum, No. 0179, funded by the Deutsche Forschungsgemeinschaft.

References

Alldredge, A., Passow, U., and Logan, B. E.: The abundance and significance of a class of large, transparent organic particles in the ocean, Deep-Sea Res. I, 40, 1131–1140, 1993.

Alldredge, A. and Silver, M.: Characteristics, dynamics and significance of marine snow, Prog. Oceanogr., 20, 41–82, 1988.

Alldredge, A. and Gotschalk, C. C.: Direct observations of the mass flocculation of diatom blooms: characteristics, settling velocities and formation of diatom aggregates, Deep-Sea Res. I, 36, 159–171, 1989.

Angel, M. V.: Detrital organic fluxes through pelagic ecosystems, in: Flows of energy and materials in marine ecosystems, edited by: Fasham, M. J. R., Plenum Press, New York, 475–516, 1984.

Angel, M. V.: Does mesopelagic biology affect vertical flux?, in: Productivity of the Ocean: Past and Present, edited by: Berger, W. H., Smetacek, V. S., and Wefer, G., J. Wiley and Sons, Chichester, 155–173, 1989.

Armstrong, R. A., Lee, C., Hedges, J. I., et al.: A new, mechanistic model of organic carbon fluxes in the ocean based on the quantitative association of POC with ballast minerals, Deep-Sea Res. II, 49, 219–236, 2002.

Asper, V. L.: Measuring the flux and sinking speed of marine snow aggregates, Deep-Sea Res. I, 34, 1–17, 1987.

Asper, V. and Smith, W. O.: Abundance, distribution and sinking rates of aggregates in the Ross Sea, Antarctica, Deep-Sea Res. I, 50, 131–150, 2003.

Berelson, W. M.: Particle settling rates increase with depth in the ocean, Deep-Sea Res. II, 49, 237–251, 2002.
Berner, R. A. and Honjo, S.: Pelagic sedimentation of aragonite: its geochemical significance, Science, 211, 940–942, 1981.
Billet, D. S. M., Lampitt, R. S., Rice, A. L., and Mantoura, R. F. C.: Seasonal sedimenation of phytoplankton to the deep sea benthos, Nature, 302, 520–522, 1983.
Boyd, P. W. and Trull, T. W.: Understanding the export of biogenic particles in oceanic waters: Is there consensus?, Prog. Oceanogr., 72, 276–312, 2007.
Boyer, T. P., Stephens, C., Antonov, J. I., et al.: World Ocean Atlas 2001, Volume 1: Salinity, edited by: Levitus, S., NOAA Atlas NESDIS 50, U.S. Government Printing Office, Washington, D.C., 165 pp., 2002.
Broecker, W. S.: Ocean chemistry during glacial time, Geochim. Cosmochim. Acta, 46, 1689–1705, 1982.
Cadée, G. C., Gonzalez, H., and Schnack-Schiel, S. B.: Krill diet affects faecal string settling, Polar Biol., 12, 75–80, 1992.
Cherry, R. D., Higgo, J. J. W., and Fowler, S. W.: Zooplankton fecal pellets and element residence times in the ocean, Nature, 274, 246–248, 1978.
Da Silva, A., Young, C., and Levitus, S.: Atlas of Surface Marine Data 1994, Vols. 1–5, NOAA Atlas NESDIS 6-10, US Government Printing Office, Washington, D.C., 1994.
De La Rocha, C. L. and Passow, U.: Factors influencing the sinking of POC and the efficiency of the biological pump, Deep-Sea Res. II, 54, 639–658, 2007.
Dierks, A. R. and Asper, V. L.: In situ settling speeds of marine snow aggregates below the mixed layer: Black Sea and Gulf of Mexico, Deep-Sea Res., 44, 385–398, 1997.
Fischer, G. and Wefer, G.: Long-term observations of particle fluxes in the Eastern Atlantic: seasonality, changes of flux with depth and comparison with the sediment record, in: The South Atlantic: Present and Past Circulation, edited by: Wefer, G., Berger, W. H., Siedler, G., and Webb, D. J., Springer, Berlin, 325–344, 1996.
Fischer, G., Donner, B., Ratmeyer, V., Davenport, R., and Wefer, G.: Distinct year-to-year flux variations off Cape Blanc during 1988–1991: relationship to δ^{18}O-deduced sea-surface temperatures and trade winds, J. Mar. Res., 54, 73–98, 1996a.
Fischer, G., Neuer, S., Wefer, G., and Krause, G.: Short-term sedimentation pulses recorded with a fluorescence sensor and sediment traps at 900 m depth in the Canary Basin, Limnol. Oceanogr., 41, 1354–1359, 1996b.

Fischer, G., Ratmeyer, V., and Wefer, G.: Organic carbon fluxes in the Atlantic and the Southern Ocean: relationship to primary production compiled from satellite radiometer data, Deep-Sea Res., 47, 1961–1997, 2000.
Fischer, G., Gersonde, R., and Wefer, G.: Organic carbon, biogenic silica and diatom fluxes in the marginal winter sea-ice zone and in the Polar Front Region: interannual variations and differences in composition, Deep-Sea Res. II, 49, 1721–1745, 2002.
Fischer, G., Neuer, S., Davenport, R., et al.: The Northwest African Margin, in: CMTT volume, edited by: Liu, K.-K., Atkinson, L., Quinones, R., et al., Springer, New York, in press, 2008.
Fowler, S. W. and Small, W. F.: Sinking rates of euphausiid fecal pellets, Limnol. Oceanogr., 17, 293–296, 1972.
Fowler, S. W. and Knauer, D. A.: The role of large particles in the transport of elements and organic components through the water column, Prog. Oceanogr., 16, 147–194, 1986.
Francois, R., Honjo, S., Krishfield, R., and Manganini, S.: Factors controlling the flux of organic carbon in the bathypelagic ocean, Global Biogeochem. Cy., 16, 1087, doi:10.1029/2001GB001722, 2002.
Gehlen, M., Bopp, L., Emprin, N., Aumont, O., Heinze, C., and Ragueneau, O.: Reconciling surface ocean productivity, export fluxes and sediment composition in a global biogeochemical ocean model, Biogeosciences, 3, 521–537, 2006, http://www.biogeosciences.net/3/521/2006/.
Gorsky, G., Le Borgne, R., Picheral, M., and Stemmann, L.: Marine snow latitudinal distribution in the equatorial Pacific along 180°, J. Geophys. Res., 108, 8146, doi:10.1029/2001JC001064, 2003.
Gohin, F., Druon, J. N., and Lampert, L.: A five channel chlorophyll concentration algorithm applied to SeaWIFS data processed by SeaDAS in coastal waters, Int. J. Remote Sens., 23, 1639–1661, 2002.
Gruber, N., Frenzel, H., Doney, S. C., et al.: Eddy-resolving simulation of phytoplankton ecosystem dynamics in the California Current, Deep-Sea Res. I, 53, 1483–1516, 2006.
Hamm, C. E.: Interactive aggregation and sedimentation of diatoms and clay-sized lithogenic material, Limnol. Oceanogr., 47, 1790–1795, 2002.
Harding, L. W., Magnuson, A., and Mallonee, M. E.: SeaWiFS retrievals of chlorophyll in Chesapeake Bay and the mid-Atlantic bight, Estuarine Coastal Shelf Sci., 62, 75–94, 2005.
Helmke, P., Romero, O., and Fischer, G.: Northwest African upwelling and its effect on off-shore organic carbon export to the deep sea, Global Biogeochem. Cy., 19, GB4015,

doi:10.1029/2004GB002265, 2005.
Honjo, S.: Coccoliths: production, transportation and sedimentation, Mar. Micropaleont., 1, 65–79, 1976.
Honjo, S.: Seasonality and interaction of biogenic and lithogenic particulate flux in the Panama Basin, Science, 218, 883–884, 1982.
Intergovernmental Oceanographic Commission, International Hydrographic Organization, and British Oceanographic Data Centre (IOC, IHO, and BODC): Centenary Edition of the GEBCO Digital Atlas on Behalf of the Intergovernmental Oceanographic Commission and the International Hydrographic Organization as Part of the General Bathymetric Chart of the Oceans, CD-ROM, Liverpool, UK, 2003.
Ittekkot, V.: The abiotically driven biological pump in the ocean and short-term fluctuations in atmospheric CO_2 contents, Global Planet. Change, 8, 17–25, 1993.
Jackson, G. A.: Effect of coagulation on a model planktonic food web, Deep-Sea Res. I, 48, 95–123, 2001.
Jackson, G. A.: Coagulation theory and models of oceanic plankton, in: Flocculation in Natural and Engineered Environmental Systems, edited by: Droppo, I., Leppard, G., Liss, S., and Milligan, T., CRC Press, Boca Raton, FL, 271–292, 2005.
Kanamitsu, M., Ebisuzaki, W., Woollen, J., Yang, S.-K., Hnilo, J. J., Fiorion, M., and Potter, J.: NCEP-DOE AMIP-II Reanalysis (R-2), Bull. Am. Meteorol. Soc., 83, 1631–1643, 2002.
Karakas, G., Nowald, N., Blaas, M., et al.: High-resolution modelling of sediment erosion and particle transport across the NW African shelf, J. Geophys. Res., 111, C06025, doi:10.1029/2005JC003296, 2006.
Klaas, C. and Archer, D. E.: Association of sinking organic matter with various types of ballast in the deep sea: Implications for the rain ratio, Global Biogeochem. Cy., 16, 1116, doi:10.1029/2001GB001765, 2002.
Knappertsbusch, M. and Brummer, G.-J.: A sediment trap investigation of sinking coccolithophorids in the North Atlantic, Deep-Sea Res. I, 47, 1083–1109, 1995.
Kremling, K., Lentz, U., Zeitzschel, B., et al.: New type of time-series sediment trap for the reliable collection of inorganic and organic trace chemical substances, Rev. Scient. Instr., 67, 4360–4363, 1996.
Kriest, I.: Different parameterizations of marine snow in a 1D-model and their influence on representation of marine snow, nitrogen budget and sedimentation, Deep Sea Res., 49, 2133–2162, 2002.

Lavender, S. J., Pinkerton, M. H., Froidefond, J. M., Morales, J., Aiken, J., and Moore, G. F.: SeaWiFS validation in European coastal waters using optical and bio-geochemical measurements, Int. J. Remote Sens., 25, 1481–1488, 2004.

Legendre, L. and Rivkin, R.: Fluxes of carbon in the upper ocean: regulation by food web control modes, Mar. Ecol., 242, 95–109, 2002.

Marchesiello, P. and Estrade, P.: Eddy activity and mixing in upwelling systems: a comparative study of Northwest Africa and California regions, Int. J. Earth Sci., doi:10.1007/s00531-007-0235-6, 2007.

Müller, P. J. and Fischer, G.: A 4-year sediment trap record of alkenones from the filamentous upwelling region off Cape Blanc, NW Africa and a comparison with distributions in underlying sediments, Deep-Sea Res. I, 48, 1877–1903, 2001.

Müller, P. J. and Fischer, G.: C37-alkenones as paleotemperature tool: fundamentals based in sediment traps and surface sediments from the South Atlantic Ocean, in: The South Atlantic in the Late Quaternary: Reconstruction of material budgets and current systems, edited by: Wefer, G., Mulitza, S., and Ratmeyer, V., Springer, Berlin, Heidelberg, New York, 167–193, 2003.

Müller, P. J. and Schneider, R.: An automated leaching method for the determination of opal in sediments and particulate matter, Deep-Sea Res. I, 40, 425–444, 1993.

Neuer, S., Ratmeyer, V., Davenport, R., et al.: Deep water particle flux in the Canary Island region: seasonal trends in relation to long-term satellite derived pigment data and lateral sources, Deep-Sea Res., 44, 1451–1466, 1997.

Neuer, S., Freudenthal, T., Davenport, R., et al.: Seasonality of surface water properties and particle flux along a productivity gradient off NW Africa, Deep-Sea Res. II, 49, 3561–3576, 2002.

Nowald, N., Karakas, G., Ratmeyer, V., Fischer, G., Schlitzer, R., Davenport, R. A., and Wefer, G.: Distribution and transport processes of marine particulate matter off Cape Blanc (NW-Africa): results from vertical camera profiles, Ocean Sci. Discuss., 3, 903–938, 2006, http://www.ocean-sci-discuss.net/3/903/2006/.

Passow, U.: Switching perspectives: Do mineral fluxes determine particulate organic fluxes or vice versa, Geochem. Geophys. Geosyst., 5, Q04002, doi:10.1029/2003GC000670, 2004.

Pilskaln, C. H. and Honjo, S.: The fecal pellet fraction of biogeochemical fluxes to the deep sea, Global Biogeochem. Cy., 1, 31–48, 1987.

Pilskaln, C. H., Lehmann, C., Padaun, J. B., and Silver, M. W.: Spatial and temporal dynamics

in marine aggregate abundance, sinking rate and flux: Monterey Bay, California, Deep-Sea Res. II, 45, 1803–1837, 1998.
Ploug, H., Iversen, M., Koski, M., and Buitenhuis, E. T.: Production, oxygen respiration rates and sinking velocity of copepod fecal pellets: direct measurements of ballasting by opal and calcite, Limnol. Oceanogr., in press, 2008.
Reynolds, R. W. and Smith, T. M.: Improved global sea surface temperature analyses using optimum interpolation, J. Climate, 7, 929–948, 1994.
Riebesell, U.: The formation of large marine snow and its sustained residence time in surface waters, Limnol. Oceanogr., 37, 63–76, 1992.
Sawada, K., Handa, N., and Nakatsuka, T.: Production and transport of long-chain alkenones and alkyl alkenoates in a sea water column in the northwestern Pacific off central Japan, Mar. Chem., 59, 219–234, 1998.
Schiebel, R.: Planktic foraminiferal sedimentation and the marine calcite budget, Global Biogeochem. Cy., 16, doi:10.1029/2001GB001459, 2002.
Scholten, J. C., Fietzke, J., Vogler, S., et al.: Trapping efficiencies of sediment traps from the deep Eastern North Atlantic: the ^{230}Th calibration, Deep-Sea Res. II, 48, 2383–2408, 2001.
Shchepetkin, A. F. and McWilliams, J. C.: Quasi-monotone advection schemes based on explicit locally adaptive disspiation, Mon. Weather Rev., 126, 1541–1580, 1998.
Shchepetkin, A. F. and McWilliams, J. C.: A method for computing horizontal pressure-gradient force in an oceanic model with a nonaligned vertical coordinate, J. Geophys. Res., 108(C3), 3090, doi:10.1029/2001JC001047, 2003.
Shchepetkin, A. F. and McWilliams, J. C.: The regional oceanic modeling system (ROMS): a split-explicit, free-surface, topography-following-coordinate oceanic model, Ocean Model., 9(4), 347–404, 2005.
Smetacek, V. S.: Role of sinking in diatom life-history cycles: ecological, evolutionary and geological significance, Mar. Biol., 84, 239–251, 1985.
Stemmann, L., Jackson, G. A., and Ianson, D.: A vertical model of particle size distributions and fluxes in the midwater column that indicates biological and physical processes – part I: model formulation, Deep-Sea Res. I, 51, 865–884, 2004.
Stephens, C., Antonov, J. I., Boyer, T. P., et al.: World Ocean Atlas 2001, Volume 1: Temperature, edited by: Levitus, S., NOAA Atlas NESDIS 49, U.S. Government Printing Office, Washington, D.C., 167 pp., 2002.
Turner, J. T.: Zooplankton fecal pellets, marine snow and sinking phytoplankton blooms, Aquat.

Microb. Ecol., 27, 57–102, 2002.
Yu, E. F., Francois, R., Honjo, S., Fleer, A. P., Manganini, S. J., Rutgers van der Loeff, M. M., and Ittekot, V.: Trapping efficiency of bottom-tethered sediment traps estimated from the intercepted fluxes of ^{230}Th and ^{231}Pa, Deep-Sea Res. I, 48, 865–889, 2001.
Wefer, G., Fischer, G., Fütterer, D., and Gersonde, R.: Seasonal particle flux in the Bransfield Strait, Antarctica, Deep-Sea Res. I, 35, 891–898, 1988.

Table 1. Sinking rates of particles in the Atlantic Ocean based on seasonal data, using the correlation and the major-peak method (Berelson, 2002). Trap data are shown on the left. Mean sinking rates for each area and the normalized values (19.6 days) are also given, accounting for the variable sampling intervals (9.5 to 30 days). Important references are also given. EAA = Eastern Equatorial Atlantic, WEA = Western Equatorial Atlantic. Locations of trapping sites are shown in Fig. 1.

Table 1.

Area	Location	Deploy-ment	Year	Lat/Long	Trap depth m upper	Trap depth m lower	Cup interval days	m. peak lag cups	m. peak lag days	season/month	s. r. m. peak m d^{-1}	norm. s. r. m. peak m d^{-1}	corr. m. r^2 no shift	r^2 1-cup	r^2 2-cup	data points	s. r. corr. m. m d^{-1}	norm. s. r. corr. m. m d^{-1}	Basic reference
Canary Current	Cape Blanc	CB3	1990	20°10 N/21°40 W	730	3557	21.5	0	10.75	spr 90	**263**	298	**0.99**	–	–	3	**263**	288	Fischer et al. (1996)
					730	3557	21.5	0	10.75	su 90	**263**	298	**0.40**	–	–	4	**263**	288	
		CB4	1991	21°09 N/20°41 W	733	3562	10	1	10	su 91	**283**	149	0.31	**0.43**	–	9	**283**	144	Fischer et al. (1996)
		CB7	1995/97	21°15 N/20°42 W	755	3586	22	0	11	wi 95	**257**	298	**0.92**	0.21	–	4	**257**	289	unpublished data
		CB13	2002/3	21°16 N/20°46 W	1228	3606	19	1	19	spr 02	**125**	125	**0.84**	0.76	–	4	**250**	243	unpublished data
					1228	3606	19	0	9.5	su 02	**250**	250	**0.82**	0.01	–	4	**250**	243	
					1228	3606	19	–	–	fall 02	**–**	–	**0.81**	0.01	–	4	**250**	243	
					1228	3606	19	–	–	wi–spr 02/03	**–**	–	0.06	0.24	**0.69**	5	**63**	61	
	Cape Verde I.	CV1	1992/93	11°29 N/21°01 W	1003	4523	9.5	1	9.5	wi 93	**371**	185	**0.40**	–	–	10	**741**	359	Fischer and Wefer (1996)
		CV2	1993/94	11°29 N/21°03 W	975	4435	25	1	25	spr–su 93	**138**	182	0.23	**0.60**	–	7	**91**	177	Ratmeyer et al. (1999)
E' Equatorial A. eastern (11° W)	EEA 2° N	GBN3	1989/90	01°47 N/11°07 W	853	3921	19.5	0	9.75	wi–spr 89	**315**	323	**0.80**	0.68	–	6	**315**	313	Fischer and Wefer (1996)
					853	3921	19.5	0	9.75	su 89	**315**	323	**0.92**	–	–	5	**315**	313	
	EEA 0° (EQ)	EA9	1992/93	00°01 N/10°48 W	1226	3786	9.5	0	4.75	fall 92	**539**	269	**0.06**	0.01	–	8	**–**	–	unpublished data
		EA7	1991/92	00°03 S/10°49 W	949	4029	15.4	0	7.7	wi 91/92	**400**	324	**0.44**	–	–	6	**400**	314	unpublished data
	EEA 2° S	GBS5	1990/91	02°11 S/09°55 W	597	3382	29.6	0	14.8	fall 90	**188**	293	**0.50**	0.06	–	4	**188**	284	Fischer and Wefer (1996)
	EEA 5° S	EA8	1991/92	05°47 S/09°25 W	588	1833	15.4	0	7.7	wi 91/92	**162**	131	**0.76**	0.22	–	5	**162**	127	Müller and Fischer (2001)
					588	1833	15.4	0	7.7	spr 92	**162**	131	**0.63**	0.08	–	6	**162**	127	
					588	1833	15.4	0	7.7	su 92	**162**	131	**0.72**	0.07	–	6	**162**	127	
					1833	2890	15.4	1	15.4	wi 91/92	**69**	56	**0.54**	0.15	–	5	**137**	108	
					1833	2890	15.4	1	15.4	spr 92	**69**	56	**0.77**	0.21	–	6	**137**	108	
					1833	2890	15.4	0	7.7	su 92	**137**	111	**0.81**	0.76	–	6	**137**	108	
					588	2890	15.4	1	15.4	wi 91/92	**149**	121	0.19	**0.92**	–	5	**149**	117	
					588	2890	15.4	1	15.4	spr 92	**149**	121	**0.58**	0.03	–	6	**299**	235	
					588	2890	15.4	0	7.7	su 92	**299**	242	**0.40**	0.31		6	**299**	235	
W' Equatorial A. western (25° W)	WEA 0° (EQ)	WA8	1994–1996	00°01 N/23°27 W	718	3204	28	1	28	fall–wi 94/95	**89**	131	0.12	**0.55**	–	8	**89**	127	unpublished data
		WA11	1996/97	00°01 S/23°25 W	834	3318	17	0	8.5	spr 96	**292**	261	**0.89**	–	–	6	**292**	253	unpublished data
		WA19	2001/02	00°06 N/23°27 W	926	3184	20.5	0	10.25	su–fall 01	**220**	238	0.19	**0.25**	0.23	9	**110**	115	unpublished data
	WEA 4° S	WA4	1993/94	03°59 S/25°35 W	808	4555	25	1	25	spr 93	**150**	197	–	**0.93**	–	5	**150**	191	unpublished data
					808	4555	25	1	25	spr 94	**150**	197	0.19	**0.46**	–	5	**150**	191	
		WA7	1994–1996	03°58 S/25°39 W	854	4630	28	0	14.5	fall 94–su 95	**260**	397	**0.52**	–	–	12	**260**	385	unpublished data
		WA10	1996/97	03°55 S/25°41 W	800	4585	17	2	34	su–fall 96	**111**	105	–	–	**0.69**	10	**111**	97	unpublished data
	WEA 7° S	WA9	1996/97	07°28 S/28°09 W	591	4451	17	0	8.5	su 96	**454**	406	**0.95**	0.01	–	6	**454**	394	unpublished data
		WA13	1997/98	07°28 S/28°14 W	871	4736	22.5	1	22.5	spr–su 97	**172**	203	0.20	**0.45**	–	9	**172**	197	unpublished data
		WA14	1998/99	07°28 S/28°14 W	833	4705	27.5	0	13.75	su–fall 98	**282**	408	**0.42**	0.02	–	7	**282**	395	unpublished data
					833	4705	27.5	0	13.75	su–fall 99	**282**	408	0.05	0.09	–	6	**–**	–	
Benguela Current	Walvis Ridge	WR2	1989/90	20°02 S/09°09 E	599	1648	18	0	9	austral fall 89	**117**	110	**0.95**	0.01	–	5	**117**	107	Fischer and Wefer (1996)
Southern Ocean	Bouvet Island	BO3	1992–1994	54°20 S/03°18 W	507	2244	23	0	11.5	austral spr–su 92/93	**151**	183	**0.82**	0.44	–	4	**151**	177	Fischer et al. (2002)
	Polar Front	PF3	1989/90	50°07 S/05°50 E	614	3196	21	1	21	Dec–Jan 89/90	**123**	136	–	–	–	–			Fischer et al. (2002)
					614	3196	21	0	10.5	Feb–Mar 90	**246**	272	**0.38**	–	–	4	**246**	263	
	Bransfield S.	KG1	1983/84	62°15 S/57°31 W	494	1588	30	0	15	austral spr–su 83/84	**73**	58	**0.99**	–	–	3	**73**	112	Wefer and Fischer (1988)

s. r. = sinking rates, norm. = normalized, m. peak = major peak method, corr. m. = correlation method

BGD

5, 2541–2581, 2008

Table 2. Sinking rates of particles calculated from alkenone measurements from the Cape Blanc deployments (at site CB; Müller and Fischer, 2001, and unpublished data). Note the increase of mean sinking rates with depth (from 51 to 108 to 318 m d^{-1}) and the extraordinary high rates in 1991 (CB-4) during the sedimentation of a coccolithophorid bloom.

Trap deployment year	CB1 1988	CB2 1989	CB3 1990/91	CB3 1990/91	CB3 1990/91	CB4 1991	CB4 1991	CB4 1991	CB13 2002/03	CB13 2002/03	CB13 2002/03
lag of peaks (cup) lag of peaks (days)	– 25	– 45	– 48	– 48	0 10.75	– 10	– 10	0 5	– 19	– 36	1 19
season	summer	summer	summer	summer	summer	summer	summer	summer	late summer	late w./late su	late w./late su
depths (m)	0 2195	0 3502	0 730	0 3557	730 3557	0 733	0 3562	733 3562	0 1228	0 3606	1228 3606
sinking rates (m day^{-1})	**88**	**78**	**15**	**74**	**263**	**73**	**356**	**566**	**65**	**100**	**125**
sampling intervals (days)	*27*	*17*	*21.5*	*21.5*	*21.5*	*10*	*10*	*10*	*19*	*19*	*19*
Reference	Müller and Fischer (2001)	Müller and Fischer (2001)	Müller and Fischer (2001)	Müller and Fischer (2001)	Müller and Fischer (2001)	Müller and Fischer (2001)	Müller and Fischer (2001)	Müller and Fischer (2001)	unpublished data	unpublished data	unpublished data

BGD
5, 2541–2581, 2008

Table 3. Summary of sinking rates derived from this study (Tables 1 and 2) in comparison to literature values for fecal pellets and diatom aggregates. Values from site CV-1 were excluded (see text).

Method	Region	Study sites	Sinking rate m d^{-1} (corr. method)	Depth range m	Remark	Reference
flux patterns	Northeast Atlantic	see Table 1	**271**	984–3764 m	mean, exclude CV	this study
	Eastern Eq. Atlantik	see Table 1	**220**	964–2991 m	mean	this study
	Western Eq. Atlantik	see Table 1	**207**	807–4239 m	mean	this study
	Southeast Atlantic	WR, see Table 1	**117**	599–1648 m		this study
	Southern Ocean	see Table 1	**157**	557–2556 m	mean	this study
	Cape Blanc	CB	**235**	983–3589 m	mean	this study
	Cape Blanc	CB13	**63**	1228–3606 m	winter-spring bloom	this study
	Cape Blanc	CB13	**250**	1228–3606 m	summer	this study
flux patterns/ chlorophyll	Cape Blanc	CB9	**90**	surface to 3600 m	winter-spring bloom	from Helmke et al. (2005)
	Cape Blanc	CB9	**120**	surface to 3600m	summer	from Helmke et al. (2005)
alkenones	Cape Blanc	CB1,2,3,4,13	**51**	surface-shallow traps	Table 2, mean	this study
		CB1,2,3,4,13	**108**	surface–deep traps	Table 2, mean	
		CB1,2,3,4,13	**318**	shallow-deep traps	Table 2, mean	
	Polar Front	PF3	**9**	surface to 613 m		Müller and Fischer (2003)
	Eastern Equatorial Atlantic	EA8	**13**	Surface to 598m		Müller and Fischer (2003)
	Namibia upwelling	NU1	**45**	Surface to 2516 m		Müller and Fischer (2003)
	Walvis Ridge	WR2-4	**48**	Surface to 1648/1717 m		Müller and Fischer (2003)
alkenones	Western Pacific off Japan	–	**145–290**	surface to 8688 m	–	Sawada et al. (1998)
sediment trap fluxes	Eastern Equatorial Pacific	–	**150**	surface to 5000 m	coccol. fecal pellets	Honjo (1976)
sediment trap fluxes	Panama Basin	–	**65**	surface to 3860 m	mucus coccol. mats	Honjo (1982)
–	–	–	**100**		diatom flocs	Smetacek (1985)
settling chambers	Monterey Bay, Calif.	–	**43–95**	surface ocean	marine snow	Shanks and Trent (1980)
photography	Northeast Atlantic	–	**100–150**	surface to seafloor	diatom aggregates	Billet et al. (1983)
in situ observations	Santa B. channel, Calif.	–	**117±56**	surface	diatom flocs	Alldredge and Gotschalk (1989)

BGD
5, 2541–2581, 2008

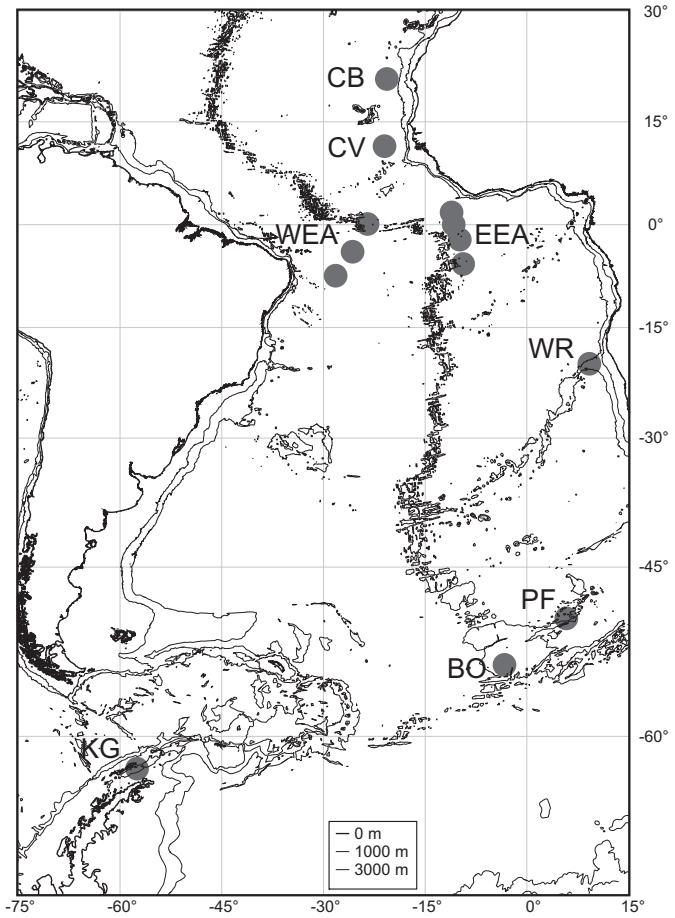

Fig. 1. Locations of the sediment trap mooring sites in the Atlantic Ocean (see Table 1). WEA = western Equatorial Atlantic, EEA = eastern Equatorial Atlantic.

BGD

5, 2541–2581, 2008

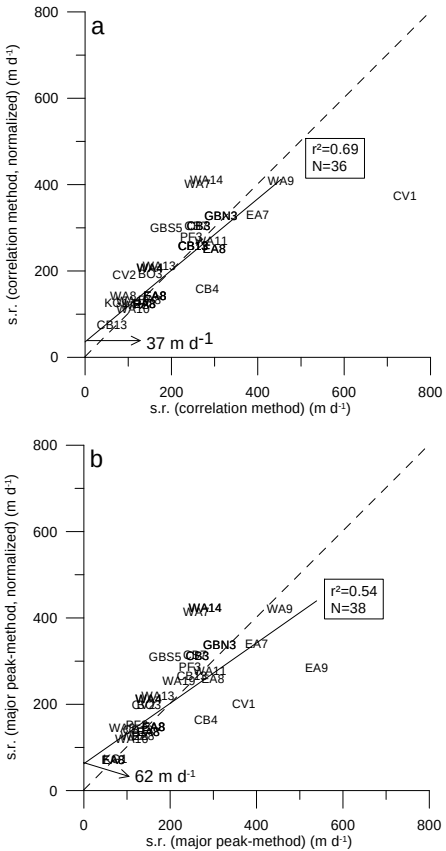

Fig. 2. Relationship between the sinking rates based on variable sampling intervals and the normalized (19.6 days) values (Table 1) for, **(a)** the correlation method, **(b)** the major peak method. Note the better coefficient for method a and the regression quite close to the 1:1 line. Only site CV-1 is far from the regression line in (a) (see text).

BGD
5, 2541–2581, 2008

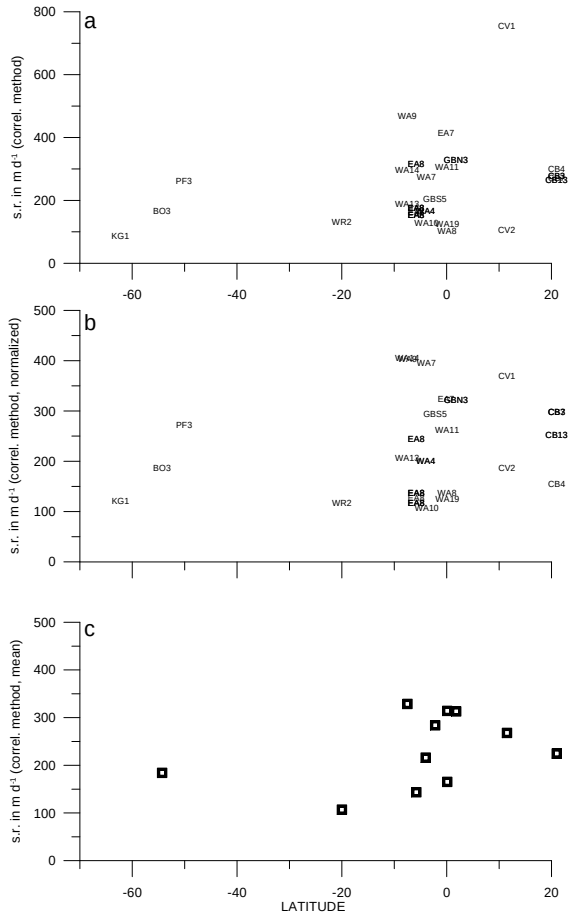

Fig. 3. Sinking rates of particles collected during different seasons in the Atlantic Ocean (Table 1, applying the correlation method) plotted vs. latitude. Raw data are shown in **(a)**, the normalized (19.6 days) are given in **(b)**, mean normalized values for each area are shown in **(c)**.

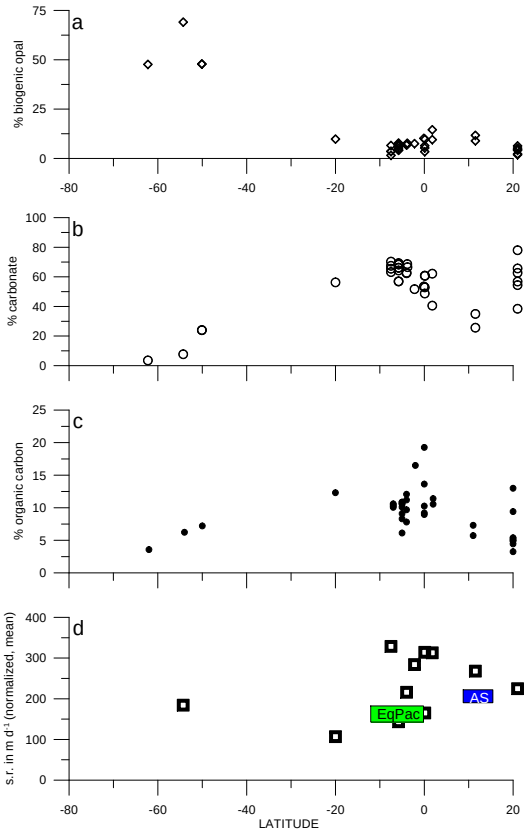

Fig. 4. Normalized mean sinking rates of particles **(d)** and particle compositions of the upper traps (**a–c**, % of total annual mass) in the Atlantic Ocean based on seasonal time resolution (Table 1). Note the high organic carbon and carbonate contents at elevated sinking rates. In (d), average sinking rates determined for the Equatorial Pacific (EqPac) and the Arabian Sea (AS) are also given (Berelson, 2002) which fit into our pattern. Note the highest mean values at and south of the Equator and off NW Africa.

BGD
5, 2541–2581, 2008

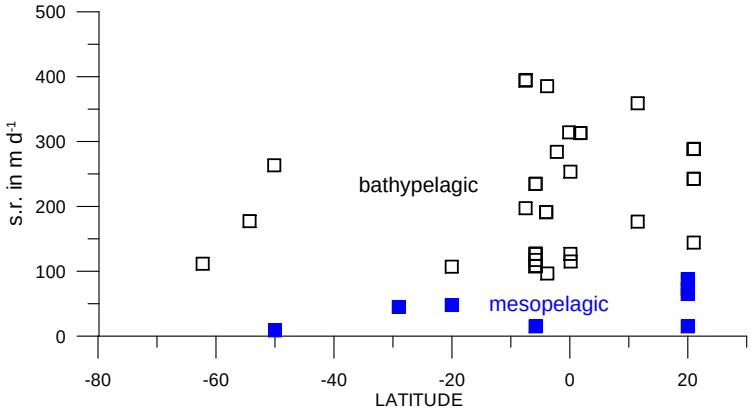

Fig. 5. Sinking rates of particles estimated for the mesopelagic zone (filled squares, from alkenone analysis, Müller and Fischer, 2001, 2003; see text) compared to sinking rates (normalized values from the correlation method, Table 1) determined from flux patterns of upper and lower traps (bathypelagic zone; open squares). Note that all sinking rates from the bathypelagic zone exceed those estimated for the upper water column suggesting increasing sinking rates with depth.

BGD
5, 2541–2581, 2008

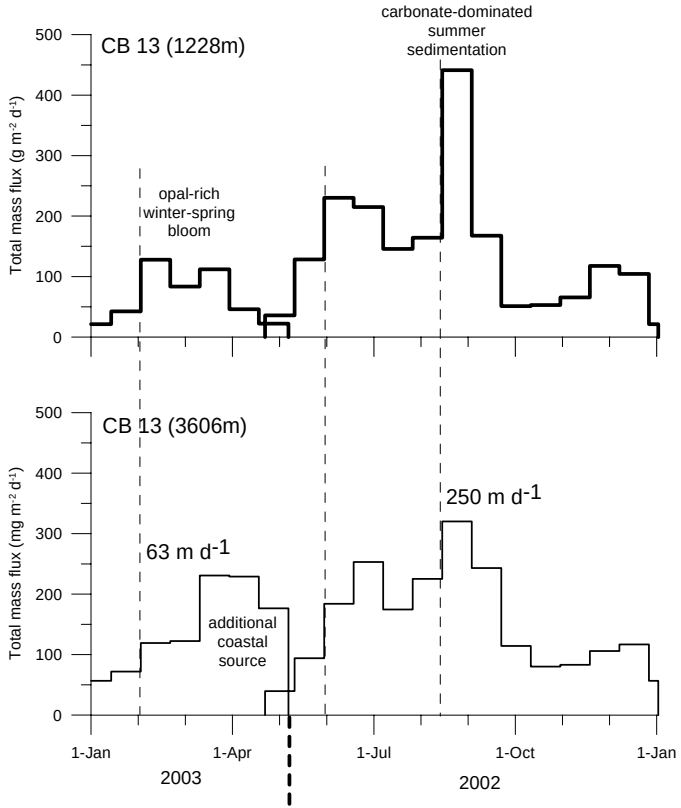

Fig. 6. Typical total mass flux patterns of upper and lower traps at the Cape Blanc site CB (deployment 13: spring 2002 to spring 2003) (Table 1). Note the shift in winter-spring combined with an increase in fluxes with depth pointing to an additional particle source at the coast (Karakas et al., 2006). A rather similar flux pattern without any delay in major peaks was observed for the late spring and summer season. Accordingly, sinking rates change from 63 m d^{-1} in spring to 250 m d^{-1} in summer.

BGD
5, 2541–2581, 2008

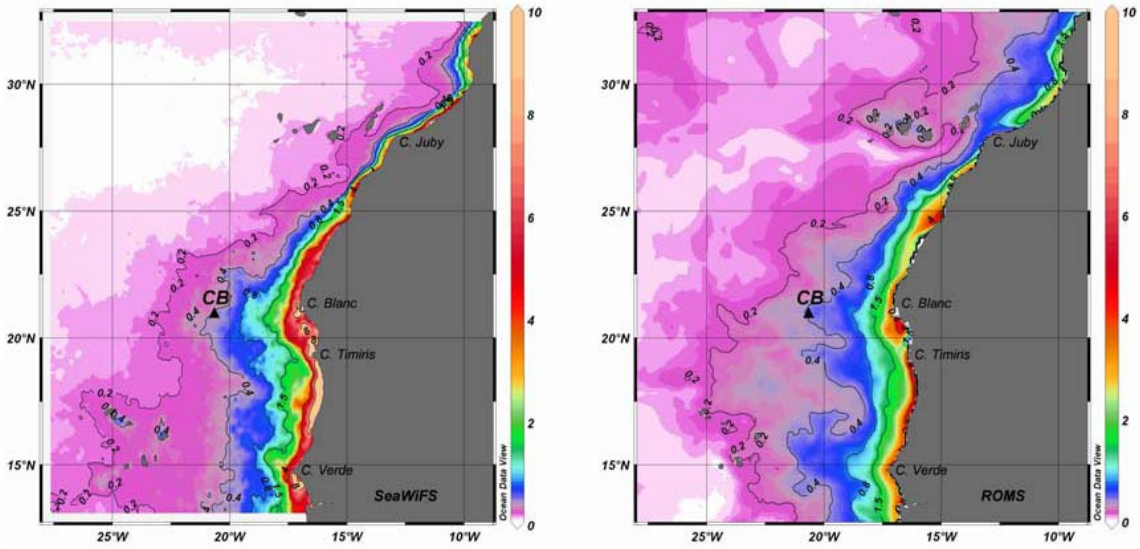

Fig. 7. Annual surface chlorophyll distribution (mg m^{-3}) as observed by SeaWiFS (left) and modelled by ROMS (right) for the year 2002.

BGD
5, 2541–2581, 2008

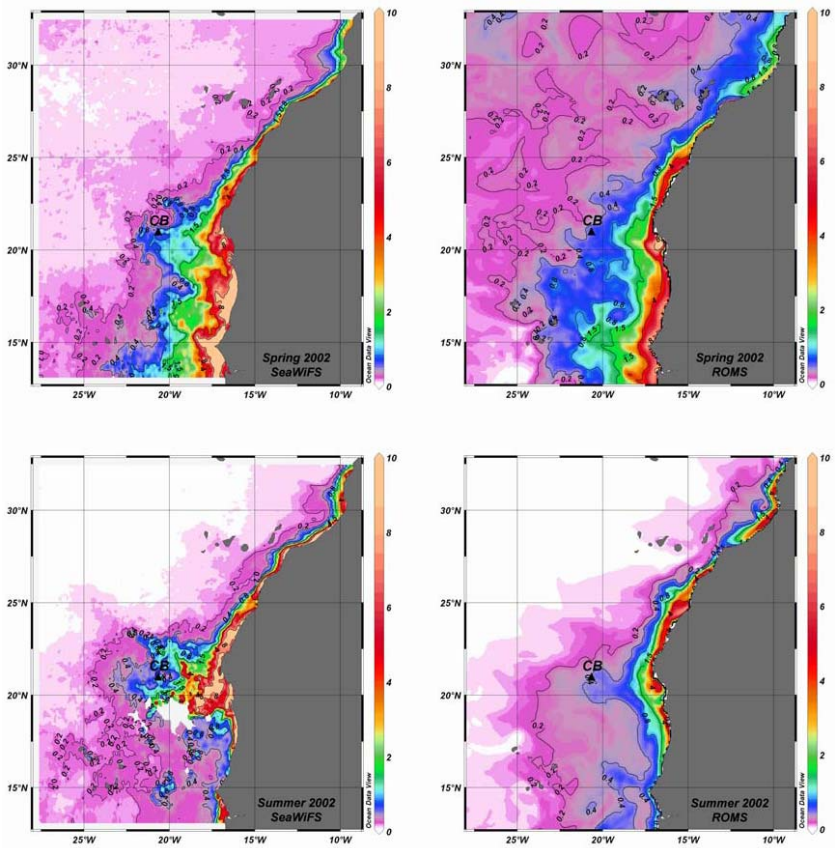

Fig. 8. (a) Seasonal surface chlorophyll distribution (mg m^{-3}) in spring (mid-March to mid-June) and summer (mid-June to mid-September) 2002 as inferred by SeaWiFS and simulated by the model.

BGD
5, 2541–2581, 2008

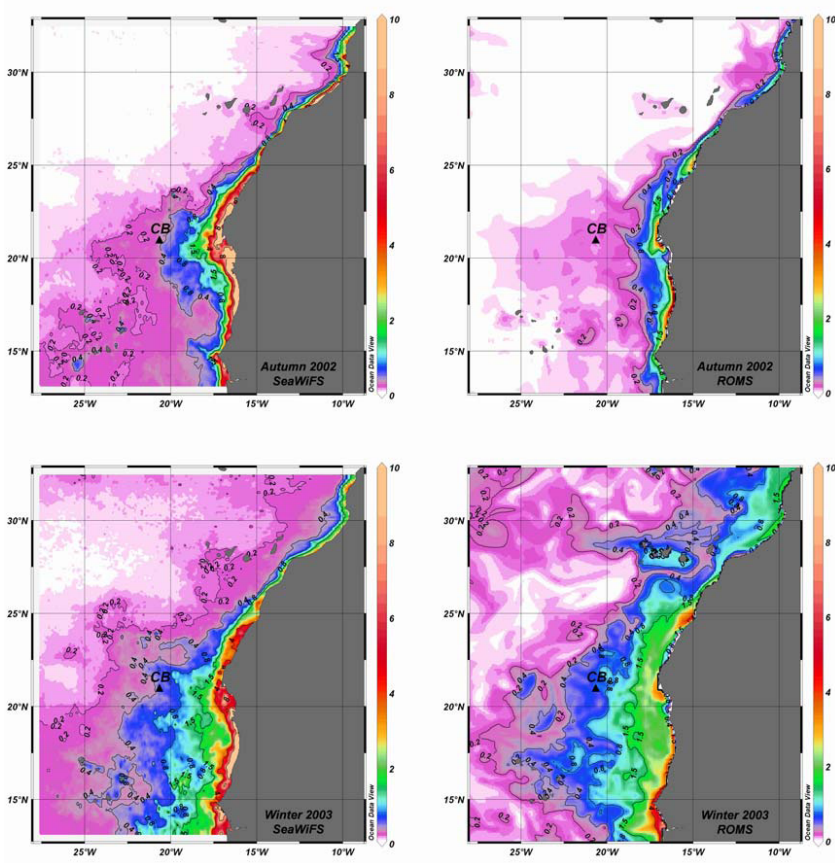

Fig. 8. (b) Seasonal surface chlorophyll distribution (mg m^{-3}) in autumn (mid-September to mid-December) 2002 and winter (mid-December to mid-March) 2003 as inferred by SeaWiFS and simulated by the model.

BGD
5, 2541–2581, 2008

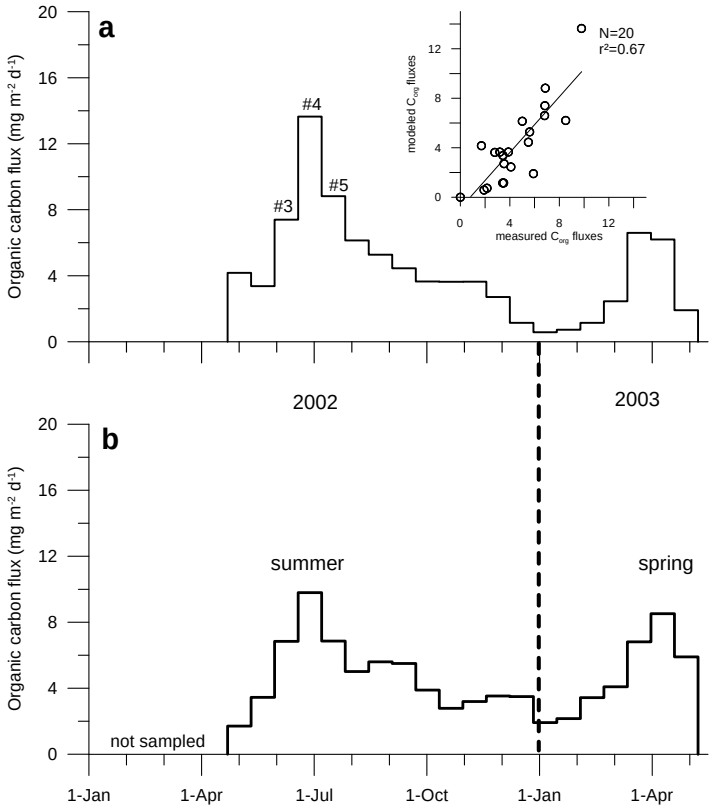

Fig. 9. Seasonal organic carbon fluxes simulated by our model **(a)** and measured with the deep ocean sediment trap CB-13 (3606 m, **b**). Sinking velocities of larger particles were set to 75 m d^{-1} in the model. In summer (samples #3 to #5), however, these values were doubled (see text and Fig. 6, Table 3). The relationship between measured and modelled organic carbon fluxes is shown as an insert in (a) (r^2=0.67, N=20).

BGD
5, 2541–2581, 2008